Journal of Enzyme Inhibition and Medicinal Chemistry, June 2009; 24(3): 753–762

An inhibition study of beauvericin on human and rat cytochrome P450 enzymes and its pharmacokinetics in rats

LI MEI[1,†], LIXIN ZHANG[2,‡], & RENKE DAI[1]

[1]*Guangzhou Institute of Biomedicine and Health, Chinese Academy of Sciences, Guangzhou 510663, China, and*
[2]*Institute of Microbiology, Chinese Academy of Sciences, Beijing 100101, China*

(*Received 21 March 2008; accepted 11 July 2008*)

Abstract
Beauvericin is a secondary metabolite natural product from microorganisms and has been shown to have a new potential antifungal activity. In this study, the metabolism and inhibition of beauvericin in human liver microsomes (HLM) and rat liver microsomes (RLM) were investigated. The apparent K_m and V_{max} of beauvericin in HLM were determined by substrate depletion approach and its inhibitory effects on cytochromes P450 (CYP) activities were evaluated using probe substrates, with IC_{50} and the (K_i) values were 1.2 μM (0.5 μM) and 1.3 μM (1.9 μM), respectively for CYP3A4/5 (midazolam) and CYP2C19 (mephenytoin). Similarly, beauvericin was also a potent inhibitor for CYP3A1/2 (IC_{50}: 1.3 μM) in RLM. Furthermore, the pharmacokinetics of beauvericin in the rat were studied after p.o administration alone and co-administration with ketoconazole, which indicated a pharmacodynamic function may play a role in the synergistic effect on antifungal activity.

Keywords: *Inhibition, cytochrome P450, beauvericin, pharmacokinetic, antifungal effect*

Introduction

Beauvericin, a cyclic lactone trimer of the amide of N-methyl L-phenylalanine and D-L-hydroxyisovaleric acid (Scheme 1), was first isolated from *Beauveria bassiana* on the basis of assays of toxicity to brineshrimp and similar to the enniatins, which are produced by a number of *Fusarium* species [1]. Recently, beauvericin has been reported to display a synergistic fungicidal effect combined with a low dosage of ketoconazole, and thereby a prospective strategy for antifungal therapy could be developed [2]. It is obvious risk that fungal infections is greatly increased in patients who are severely immuno-compromised due to cancer chemotherapy, organ or bone marrow transplantation, or through human immunodeficiency viral infections [2–5]. Additionally, new antifungal medicines are needed regarding there are more and more drug-resistant fungal infections [2,6–8]. Therefore, it is an unmet need to develop new chemicals or therapeutic application for antifungal.

A new chemical entity for clinical application should satisfy certain pharmacokinetic property, mainly revealed as the drug absorption, distribution, metabolism, and excretion (ADME) properties [9–11]. Additionally, the risk of drug interaction potentials for new drug candidate should be well evaluated before the expensive clinical trials. In the present study, the main ADME properties and pharmacokinetic property in rats for beauvericin were conducted, including the estimation of the apparent K_m and V_{max} and the inhibitory potentials of beauvericin in drug metabolizing enzymes, cytochrome P450, using specific substrates in HLM and RLM. The resulting pharmacokinetic properties in rats are also discussed.

Correspondence: R. Dai, Guangzhou Institute of Biomedicine and Health, Chinese Academy of Sciences, Guangzhou 510663, China. Tel: 86 20 32290616. E-mail: dai_renke@gibh.ac.cn

ISSN 1475-6366 print/ISSN 1475-6374 online © 2009 Informa UK Ltd.
DOI: 10.1080/14756360802362041

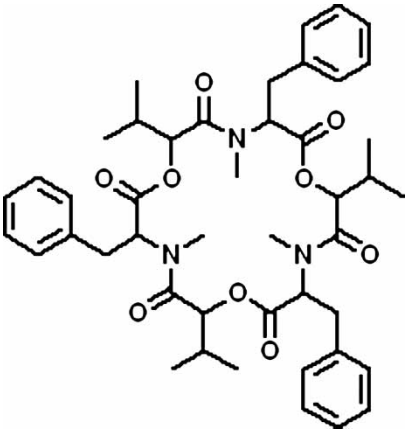

Scheme 1. The structure of beauvericin.

Materials and methods

Chemicals

Midazolam, 1′-hydroxymidazolam, mephenytoin, 4′-hydroxymephenytoin, phenytoin, dextromethorphan, dextrorphan, propranolol, α-hydroxytriazolam, henacetin, acetaminophen, salbutamol, diclofenac, 4′-hydroxydiclofenac, flufenamic acid were purchased from Sigma–Aldrich (St. Louis, MO, USA). HLM was obtained from BD Gentest (Woburn, MA). Acetonitrile, methnol (HPLC grade) was acquired from Burdick and Jackson (Muskeson, MI, USA). Formic acid (HPLC grade) were purchased from Dima technology INC., USA. Beauvericin and ketoconazole were kindly provided by Dr. Zhang Lixin (Institute of Microbiology, Chinese Academy of Sciences). Deionized water was prepared using a Mill-Q-System from Millipore Corp. (Milford, MA, USA). All other reagents and chemicals were of analytical or high-performance liquid chromatography (HPLC) grade.

LC-MS/MS conditions

Determination of all analytes was carried out using an LC/MS/MS system, which consisted of an HPLC apparatus (Shimadzu, Japan) including a SCL-10ADvp controller, two LC-10ADvp pumps and a DGU-14A solvent degasser, and a PE/SCIEX Applied Biosystems API3000 triple-quadrupole mass spectrometer (Foster City, CA, USA) equipped with electrospray ionization source. A MPS3C autosampler (GERSTEL Germany) was used for sample delivery. The HPLC columns used were a Gemini C18 110A column (2.0 × 100 mm, 5.0 μm) equipped with an ODS guard column (4 mm × 2.0 mm i.d) from Phenomenex (Torrance, CA,USA). Mobile phase of 0.1% formic acid in CH_3OH/H_2O(10/90) (A) and 0.1%formic acid in CH_3OH/H_2O(90/10) (B) were used for the chromatography in all experiments, run gradiently. Three HPLC gradient programs were designed to analyze these chemicals.

HPLC gradient program I, used for CYP2C9 and 2C19 assays, was as follows: 0 to 0.2 min, 25% B; 0.2 to 1.1 min, gradient to 90% B; 1.1to 2.0 min, 90% B; and 2.0 to 2.5 min, gradient to 25% B;

HPLC gradient program II, used for CYP3A4/5 and 2D6 assays, was as follows: 0 to 0.6 min, 10% B; 0.6 to 1.3 min, gradient to 95% B; 1.3to 2.5 min, 95% B; and 2.5 to 2.7 min, gradient to 10% B;

HPLC gradient program III, used for CYP1A2 assays and beauvericin analysis, was as follows: 0 to 0.4 min, 10% B; 0.4 to 1.5 min, gradient to 95% B; 1.5 to 3.0 min, 95% B; and 3.0 to 3.2 min, gradient to 10% B.

The run time was 3.8 min, column temperature was ambient, and the flow rate was 0.2 mL/min throughout the analyses.

The analytes were all detected by monitoring the precursor → product ion transition at unit resolution using multiple reaction monitoring (MRM) scan mode. Both analytes and their own ISs responded best to the positive ionization mode, with the protonated molecular ions $[M + H]^+$ as the major species. Product ion spectra and fragmentation pathways of Beauvericin was shown in Figure 1. The monitoring ion was set as *m/z* 784.1 / 262.3 for Beauvericin. For the five metabolites and ISs used as probes of cytochrome P450 activity, the MRM acquisitions were performed using the transition and collision energy described in previous paper [12]. Mass spectrometric conditions were optimized to obtain maximum sensitivity. The following ESI conditions were applied: drying gas (nitrogen) heated at 350°C and used at a flow rate of 6 L/min; nebulizer gas (nitrogen) at a pressure of 3.5 MPa and heated nebulizer parameters were set as follows (arbitrary units): nebulizer, 12; curtain: 8; capillary voltage was set at 4500 V. Data was acquired using the Analyst 1.4 software.

Preparation of RLM

RLM was prepared as previously described [13]. RLM prepared by several times was pooled together and the final concentration of proteins was measured to be 19 mg/mL by the method of Lowry et al. [14].

Substrate depletion experiment of beauvericin

Beauvericin (40, 100, 400, and 1000 nM, respectively) was incubated with HLM (0.2 mg/mL) in a total incubation volume of 1.5 mL. Aliquots (0.2 mL) were removed at 0, 2.5, 5, 8, 15, 22 and 30 min and terminated by addition to 0.4 mL of acetonitrile on ice containing 300 ng of phenytoin as internal standard. The resulting solution was vortex-mixed, and the supernatant was separated by centrifugation at 10,000*g* for 5 min at 4°C. Aliquots (20 μL) of the supernatant were injected into an LC/MS/MS system.

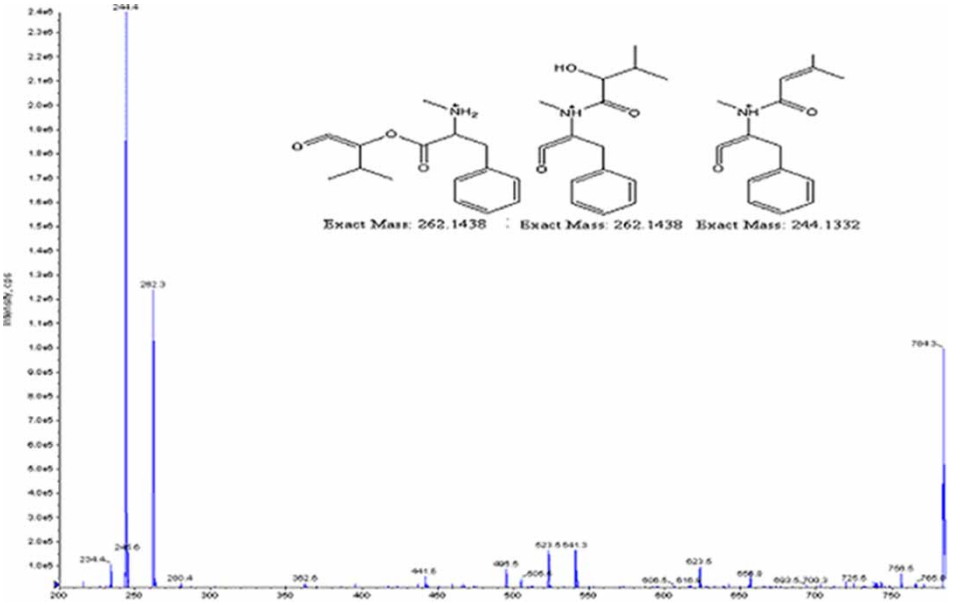

Figure 1. Full-scan product ion spectra of $[M + H]^+$ and fragmentation pathways for beauvericin.

Inhibition effect and kinetic analysis of beauvericin in HLM and RLM

In vitro *incubations*. All incubations were conducted by shaking reaction mixtures under air in a heated water bath at 37°C. Incubations were carried out in 100 mM KH_2PO_4, pH 7.4. Substrate, inhibitor, and microsomes were premixed at a certain concentration and pre-warmed for 5 min at 37°C, and incubations were commenced by addition of NADPH (1.0 mM). The final volume of the incubation mixture was 400 μL and the final concentration of organic solvent did not exceed 0.3%. After incubation at 37°C for a specific period of time, the reaction was terminated by the addition of ice-cold acetonitrile (800 μL) in which a specific amount of internal standard was contained. The resulting solution was vortex-mixed, and the supernatant was separated by centrifugation at 10,000*g* for 5 min at 4°C. Aliquots (20 μL) of the supernatant were injected into an LC/MS/MS system. In substrate saturation experiments in which product formation was measured, incubation times were set that had provided a linear reaction velocity in preliminary experiments. In substrate consumption experiments, this was intentionally not the case. All incubations were performed in duplicate, and the mean values were used for analysis.

Inhibition effects of beauvericin on the P450 Enzymes. The effect of various concentrations of beauvericin (0.05, 0.1, 0.5, 1, 10, 50 and 100 μM) on P450 activities was examined in HLM using probe substrates for corresponding specific isoforms of cytochrome P450. Five major human drug-metabolizing enzymes, CYP1A2, 2C9, 2C19, 2D6, and 3A4/5 were investigated [9]. The following activities were measured for each type of P450 enzymes: phenacetin O-deethylation for CYP1A2, mephenytoin 4′-hydroxylation for CYP2C19, dextromethorphan O-demethylation for CYP2D6, diclofenac 4′-hydroxylation for CYP2C9, and midazolam 1′-hydroxylation for CYP3A4/5. The concentrations of phenacetin, mephenytoin, dextromethorphan, diclofenac, and midazolam were set at 45, 55, 10, 10 and 5 μM respectively, all were at approximately their respective K_m values (CDER, FDA, http://www.fda.gov/cder/drug/drugInteractions/default.htm). Microsome concentrations and incubation times were all set at 0.2 mg protein/mL and 6 min respectively for each reaction, except for the isoforms of CYP2C19 in which the mephenytoin 4′-hydroxylation assay was carried in 0.3 mg protein/mL and 40 min reaction. The incubation was carried out in the same way with the method described above.

The inhibition effect of beauvericin on P450 activities in RLM was performed in a similar way with the above method for HLM. Dextromethorphan, diclofenac and midazolam were selected to be specific substrates for CYP2D2, 2C6, and 3A1/2 respectively [15]. Each incubation was performed with 0.3 mg/mL RLM.

Pharmacokinetic experiments in rats

Male Sprague–Dawley rats (8 weeks old, weighing 200–240 g) were purchased from the Laboratory Animal Services Center of Southern Medical University in China. Animals were held in wire cages under conditions of constant temperature (22–25°C), lighting (12-hr dark-light cycle) and humidity (55 ± 5%)

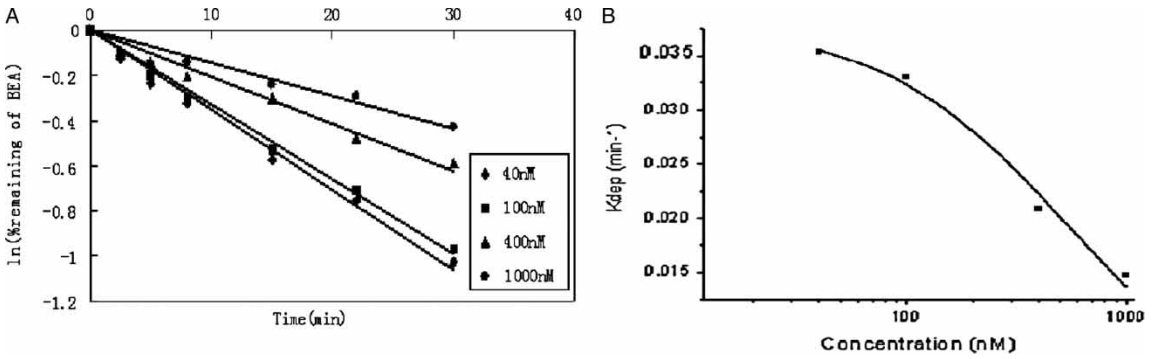

Figure 2. (A) Disappearance of beauvericin in HLM at various initial concentrations. Beauvericin at concentrations of 40, 100, 400, and 1000 nM was incubated with 0.2 mg/mL HLM. Each point represents the logarithmic value of the remaining percentage of substrate to the initial concentration in HLM. (B) Plots of *in vitro* depletion rate constants versus substrate concentration for HLM-catalyzed beauvericin metabolism. Each point represents the depletion rate constants of corresponding substrate concentration. The line represents the curve predicted from Equation (1).

with a commercial food diet and water freely available, and were acclimated in the facility for 1 week prior to testing. The animal protocols for experiments were reviewed and approved by the Institutional Laboratory Animal Care and Use Committee of Guangzhou Institute of Biomedicine and Health, Chinese Academy of Sciences.

Rats were orally dosed with 0.5, 1, and 2 mg/kg beauvericin, and co-administrated with 0.5 mg/kg ketoconazole at the dose of 0.5 mg/kg of beauvericin, respectively. Beauvericin and ketoconazole were formulated in 0.5% methylcellulose suspension before gavage. Access to water was maintained during the experiment, but animals were fasted beginning the night before the experiment. Blood samples (0.4 mL) were collected 0.133, 0.833, 1.5, 3.5, 5, 8, 12, 16 and 24 h after the dosing and immediately centrifuged at 2000 × *g* for 10 min. The plasma was then collected and stored at −80°C until analysis. For analysis, 90 μL of plasma was mixed with 10 μL of the internal standard (IS) solution (4.0 ng/mL of phenytoin) in a 1.5 mL polypropylene test tube, and then 200 μL of methnol/acetonitrile (50/50, v/v) solution was added to precipitate proteins. The mixture was vortexed for 1 min, followed by centrifugation for 10 min at 16,000*g*. A 20 μL of the supernatant was injected into the LC/MS-MS apparatus for determination of the contents interested.

Data analysis

In substrate depletion experiment, the percentage remaining versus time at each substrate concentration was fitted to first order decay functions to determine initial substrate depletion rate constants (k_{dep}). If substrate decline demonstrated nonlinearity on log percentage remaining versus time curves, only those initial timepoints wherein log-linearity was observed were used to determine depletion rate constants.

K_m values from substrate consumption experiments were determined by plotting the k_{dep} versus the substrate concentration on a linear-log plot with Origin software, version 7.5 (MicroCal Software, Inc., Northampton, MA), using the following Equation (1):

$$k_{dep} = k_{dep([S]=0)} \times \left(1 - \frac{[S]}{[S] + K_m}\right) \qquad (1)$$

in which $[S]$ is the substrate concentration, $k_{dep([S]=0)}$ represents the theoretical maximum consumption rate constant at an infinitesimally low-substrate concentration, and K_m is the Michaelis constant [16].

And the following Equation (2) was used to calculate the V_{max} values [17]:

$$V_{max} = k_{dep([S]=0)} \times K_m \qquad (2)$$

in which V_{max} is the maximum velocity of enzyme and K_m is the Michaelis constant calculated by Equation (1). Intrinsic clearance of the *in vitro* incubation was calculated as $Cl_{int} = V_{max}/K_m$.

IC_{50} values (inhibitor concentration that decreased enzyme activity by 50%) were determined by nonlinear regression of sigmoidal dose-response curves using Grafit, version 5.0. The determination of apparent K_i value (the equilibrium dissociation constant for the enzyme-inhibitor complex) was conducted from secondary reciprocal plots of apparent K_m/V_{max} (obtained from the slope of the Lineweaver-Burk plots) versus inhibitor concentration, the K_i value was equal to *x*-intercept of the secondary reciprocal plots [18,19]. Lineweaver-Burk plots and Dixon plots of the enzyme kinetic data were generated to determine the mode of inhibition [20].

The pharmacokinetic parameters were calculated using the Drug and Statistics version 2.0 software package (Anhui Provincial Center for Drug Clinical Evaluation, China).

Data were presented as the mean ± S.D. and Statistical analyses were performed by one-way analysis of variance (ANOVA), and P values of <0.05 were considered to be statistically significant.

Results

The apparent K_m and V_{max} of beauvericin in HLM determined by substrate depletion approach

To estimate the enzyme kinetic parameters of beauvericin in HLM using substrate depletion approach, each k_{dep} value at various concentrations were determined. Substrate concentrations range from 40 to 1000 nM and the depletion profiles are shown in Figure 2(A). The apparent K_m and V_{max} values for beauvericin metabolism were, therefore, estimated to be 0.6 ± 0.1 μM and 21 ± 3 nmol/min/mg-protein, respectively, according to the Equations (1) and (2) (Figure 2(B)). The intrinsic clearance value (Cl_{int}) was determined to be 38 ± 8 mL/min/mg-protein.

Inhibitory effects of beauvricin on cytochrome P450 in HLM and RLM

The inhibitory effects of beauvericin on the activities of five common major human drug-metabolizing enzymes, cytochrome P450 and three rat cytochrome P450 were evaluated, as assessed by isoform-specific probe reactions. The selective substrate concentrations were prepared near to its respective K_m value and beauvericin concentration range is from 0.05 to 100 μM. Both inhibitory results in HLM and RLM are summarized in Table I and Figure 3. Beauvericin occurred to be a strong inhibitor for midazolam 1′-hydroxylase (CYP3A4/5) and mephenytoin 4′-hydroxylase (CYP2C19) activities in HLM, with IC_{50} values of 1.2 ± 0.1 μM and 1.3 ± 0.4 μM, respectively. In contrast, Beauvericin displayed no significant inhibitory effects on the activities catalyzed by CYP1A2, 2C9, or 2D6 ($IC_{50} >$ 100 μM). Additionally, beauvericin was found to be a potent inhibitor to CYP3A1/2 with the IC_{50} value of 1.3 ± 0.6 μM and not a inhibitor at all for CYP2C6 or 2D2 in RLM ($IC_{50} > 100$ μM) as shown in Figure 4.

Table I. Inhibition effect of Beauvericin on cytochrome P450 isozyme-specific activities in HLM and RLM.

P450 Isozyme	Specific Activity	IC_{50}(S.D.) μM	K_i Mm	Mechanism of inhibition
HLM				
CYP1A2	Phenacetin *O*-deethylation	>100	–	
CYP2C9	Diclofenac 4′-Hydroxylation	>100	–	
CYP2C19	Mephenytoin 4′-Hydroxylation	1.3(0.4)	1. 9	mixed-type
CYP2D6	Dextromethorphan O-Demethylation	>100	–	
CYP3A4/5	Midazolam 1′-Hydroxylation	1.2(0.1)	0.5	competitively
RLM				
CYP3A1/2	Midazolam 1′-Hydroxylation	1.3(0.6)	–	
CYP2C6	Diclofenac 4′-Hydroxylation	>100	–	
CYP2D2	Dextromethorphan O-Demethylation	>100	–	

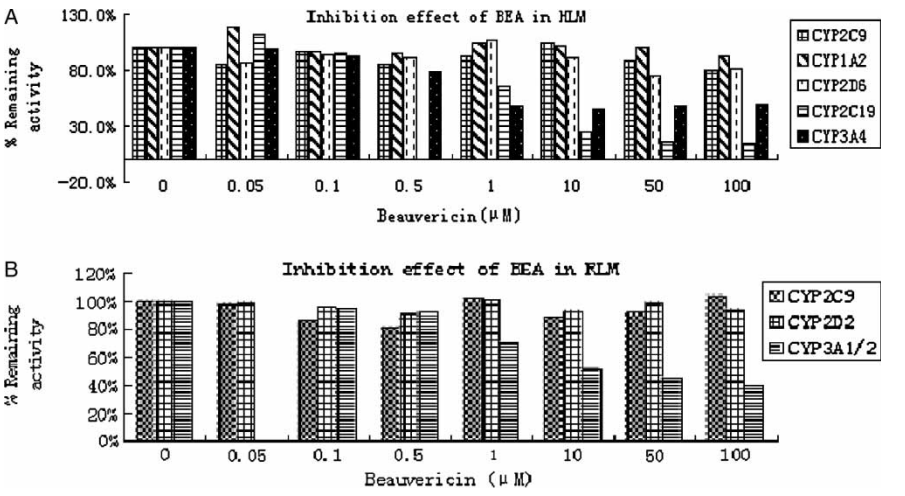

Figure 3. Inhibitory effects of beauvericin on CYP-catalyzed reactions in HLM (A) and RLM (B). Beauvericin were incubated under conditions described in Methods. The activity of each isoform was measured by isoform-specific substrate reaction probes at approximately their respective K_m value. Each data point represents the mean of duplicate experiments.

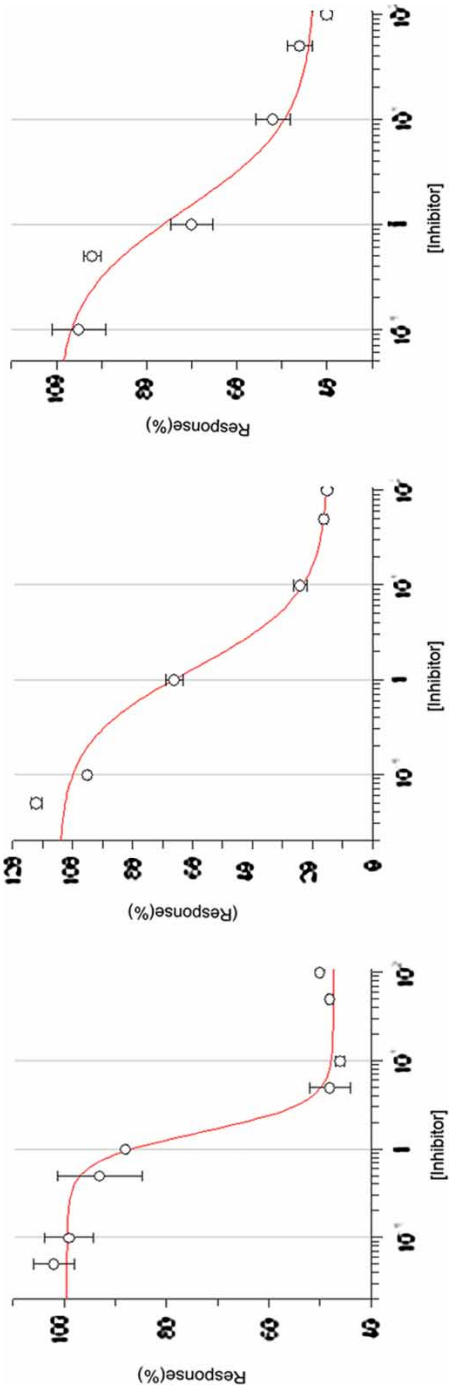

Figure 4. Inhibitory effect of beauvericin on CYP3A4/5 and 2C19 in HLM, and CYP3A1/2 in RLM for the value of IC_{50}, using the software of Grafit, version 5.0. (A) Inhibition of CYP3A4/5 (with midazolam [5 μM] as substrate) by beauvericin (0 to 100 mM) in HLM; (B) Inhibition of CYP2C19 (with mephenytoin [55 μM] as substrate) by beauvericin (0 to 100 mM) in HLM; (C)) Inhibition of CYP3A1/2 (with midazolam [5 μM] as substrate) by beauvericin (0 to 100 mM) in RLM (see Materials and Methods for details). Data are averages for duplicate incubations.

To better understand the inhibition mechanism by beauvericin, detail inhibition kinetics was conducted in HLM and revealed by Lineweaver-Burk plots, Dixon plots, and secondary reciprocal plots. Midazolam (1–5 μM) and mephenytoin (10–100 μM) were used as selective substrate of CYP3A4/5 and CYP2C19 respectively, and beauvericin (0.5–5 μM) was added to the reaction system as inhibitor. A competitive inhibition kinetics was indicated by methods of Lineweaver-Burk plot, Dixon plots, and secondary reciprocal plots for beauvericin inhibiting CYP3A4/5 activity, while a mixed type kinetics was suggested by these methods for beauvericin inhibiting CYP2C19 activity (Figure 5(A)–(F)). The apparent K_i values were calculated to be 0.5 μM and 1.9 μM for beauvericin inhibiting CYP3A4/5 and 2C19 activities, respectively, using Non-linear regression analysis.

Pharmacokinetics result of beauvericin and ketoconazole in rats

A sensitive liquid chromatography-electrospray ionization mass spectrometric (LC-MS/MS) method was established to analyze the content in rat plasma. The lower limit of detection of the method reached to 0.5 ng/mL for both beauvericin (the transition 784.1 → 262.3) and ketoconazole (the transition 531.2 → 489.4). The standard curves exhibited excellent linearity over a range of 0.5-180 ng/mL ($r^2 > 0.992$) for beauvericin and 0.5-250 ng/mL ($r^2 > 0.994$) for ketoconazole. The typical chromatograms of beauvericin in rat plasma are shown in Figure 6. The mean plasma concentration-time profiles of beauvericin after p.o. administration at the doses of 0.5, 1, and 2 mg/kg and co-administration beauvericin and ketoconazole at the doses of 0.5 mg/kg for each are shown in Figure 7.

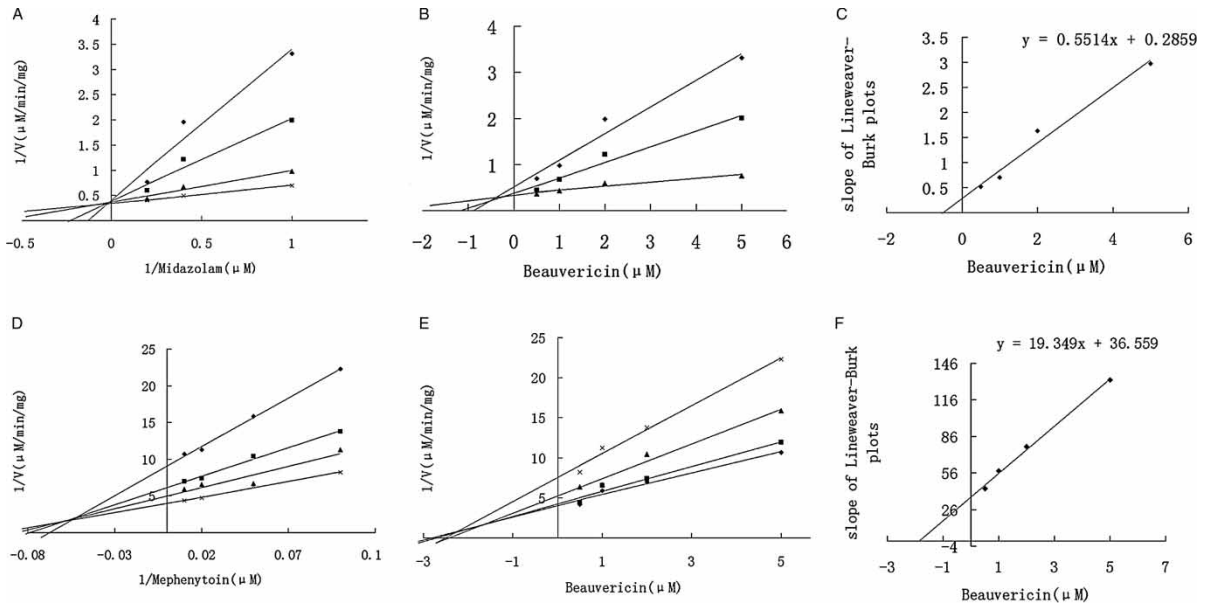

Figure 5. Lineweaver-Burk plots, Dixon plots, and secondary reciprocal plots of CYP3A4/5 catalyzed midazolam 1′-hydroxylation and CYP2C19-catalyzed mephenytoin 4′-hydroxylation by beauvericin (1–5 μM) in HLM. The symbols indicate mean of the transformed data for two independent experiments, and the lines were generated by linear regression analysis. Lineweaver-Burk plots of midazolam (A, 1–5 μM) and mephenytoin (D, 10–100 μM) in the presence of 0.5(×), 1 (▲), 2 (■), and 5 (◆) μM beauvericin. Dixon plots of midazolam (B) with 1 (◆), 2.5 (■), and 5 (▲)μM and mephenytoin (E) with 10 (×), 20 (▲), 50 (■), and 100 (◆) μM in the presence of beauvericin (0.5, 1, 2, and 5 μM). Secondary plots of the slopes taken from Lineweaver-Burk plots versus the beauvericin concentration for midazolam (C) and mephenytoin (F). Each data point represents the average of duplicate measurements.

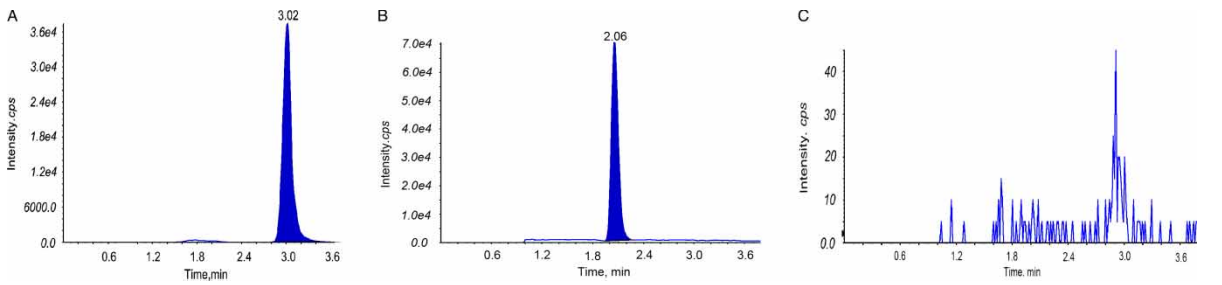

Figure 6. Typical chromatograms of beauvericin and phenytoin (internal standard, IS) in rat plasma. Plasma sample spiked with beauvericin (A) and IS (B); Blank plasma sample (C).

The pharmacokinetic parameters of these four representative doses are calculated using DAS Software and the results are shown in Table II. The results indicated that pharmacokinetic exposures for beauvericin and ketoconazole were not significantly different with the comparison of administration with each alone and with the co-administration of both.

Discussion

Biotransformation of beauvericin in HLM displayed NADPH dependency, indicating cytochrome P450 response mainly for its intrinsic clearance. Since the standards of metabolites are not readily available, the common enzyme kinetic approach monitoring the formation of metabolite(s) is not appropriate. Therefore, the substrate depletion approach is invaluable to use for determination of the apparent K_m and V_{max} of beauvericin in HLM [21–23]. The main disadvantage for this approach is that the multiple pathways may be involved in the substrate depletion and thus the resulting apparent K_m and V_{max} would be represented in a combinating contribution of multiple cytochrome P450 isoforms [23].

The apparent K_m, V_{max}, and Cl_{int} of beauvericin in HLM measured by the substrate depletion approach were determined to be 0.6 ± 0.1 μM, 21 ± 6 μM/min/mg protein, and 29 ± 14 mL/min/mg protein,

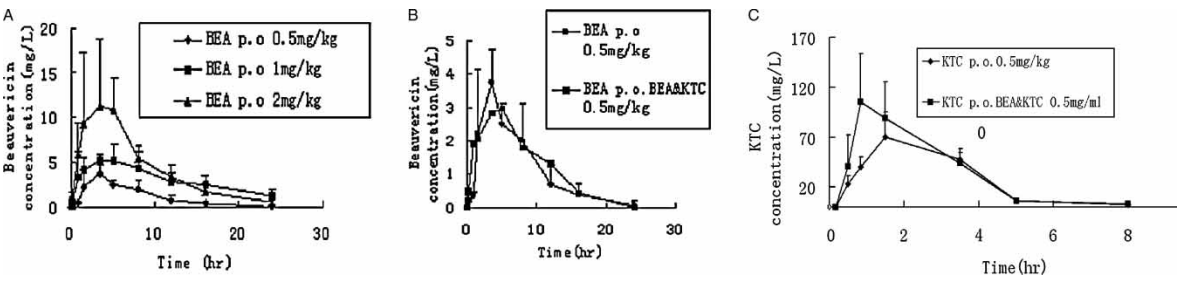

Figure 7. (A) Profiles of mean plasma concentration of beauvericin versus time after p.o. administration at the dose of 0.5, 1, 2 mg/kg. (B) Comparative profiles of mean plasma concentration of beauvericin after 0.5 mg/kg dose of beauvericin alone and co-administration with ketoconazole both at the dose of 0.5 mg/kg to rats. (C) Comparative profiles of mean plasma concentration of ketoconazole after 0.5 mg/kg dose of ketoconazole alone and co-administration with beauvericin both at the dose of 0.5 mg/kg to rats.

Table II-A. Pharmacokinetic parameters of beauvericin after oral administration to rats (n = 5; mean ± S.D.).

Parameters	Beauvericin			Beauvericin co-administered with ketoconazole (0.5 mg/kg)
	0.5 mg/kg	1.0 mg/kg	2.0 mg/kg	0.5 mg/kg
C_{max} ($mg \cdot L^{-1}$)	3.4 ± 0.4	5.4 ± 0.8	13.9 ± 4.9	3.8 ± 0.4
T_{max} (h)	4.1 ± 2.8	4.3 ± 0.8	5.4 ± 1.3	3.4 ± 0.9
MRT_{0-t} (h)	6.6 ± 1.9	9.2 ± 0.5	7.0 ± 0.9	6.3 ± 0.7
$MRT_{0-\infty}$(h)	7.5 ± 2.7	13.2 ± 2.4	7.4 ± 0.9	7.9 ± 2.5
CL_{tot} (mL/min/kg)	0.29 ± 0.06	0.21 ± 0.04	0.32 ± 0.09	0.25 ± 0.06
AUC_{0-t} ($h \cdot mg \cdot L^{-1}$)	28 ± 3	64 ± 15	101 ± 34	31 ± 6
$AUC_{0-\infty}$($h \cdot mg \cdot L^{-1}$)	29 ± 3	80 ± 21	103 ± 35	33 ± 12
$t_{1/2}$ (h)	2.9 ± 1.0	3.6 ± 1.1	3.0 ± 0.7	3.4 ± 1.7

Table II-B. Pharmacokinetic parameters of ketoconazole after oral administration to rats (n = 5; mean ± S.D.).

Parameters	Ketoconazole 0.5 mg/kg	Ketoconazole co-administered with Beauvericin (0.5 mg/kg) 0.5 mg/kg
C_{max} ($mg \cdot L^{-1}$)	70 ± 16	122 ± 35
T_{max} (h)	1.9 ± 0.6	1.1 ± 0.4
MRT_{0-t} (h)	2.4 ± 0.1	2.0 ± 0.1
$MRT_{0-\infty}$(h)	2.6 ± 0.2	2.1 ± 0.1
CL_{tot} (mL/min/kg)	0.04 ± 0.01	0.03 ± 0.01
AUC_{0-t} ($h \cdot mg \cdot L^{-1}$)	220 ± 34	309 ± 79
$AUC_{0-\infty}$($h \cdot mg \cdot L^{-1}$)	229 ± 34	313 ± 77
$t_{1/2}$ (h)	0.97 ± 0.05	0.94 ± 0.20

Data are expressed as the mean ± S.D. C_{max} ($mg \cdot L^{-1}$), maximum plasma concentration; T_{max} (h), time to reach maximum plasma concentration; MRT_{0-t} (h), mean residence time from zero up to a definite time; $MRT_{0-\infty}$(h), mean residence time from zero up to a infinite time; CL_{tot} (mL/min/kg), tota1 body clearance; AUC_{0-t} ($h \cdot mg \cdot L^{-1}$), area under the concentration–time curve from zero up to a definite time; $AUC_{0-\infty}$ ($h \cdot mg \cdot L^{-1}$), area under the concentration–time curve from zero up to a infinite time; $t_{1/2}$(h), half-time of elimination phase.

respectively, revealing high affinity of beauvericin to cytochrome P450s. These results are well correlated with the inhibition measurements of beauvericin inhibiting activities catalyzed by CYP3A4/5 and 2C19 in HLM (K_i: 0.5 μM and 1.9 μM, Table I), especially in which the competitive inhibition kinetics was determined in CYP3A4/5-mediated midazolam 1′-hydroxylation reaction. Similarly, beauvericin was found to be a potent inhibitor to CYP3A1/2 (IC_{50}: 1.3 μM) in RLM. Since the selective substrate for rat CYP2C has not been identified yet based on our knowledge, the inhibition of beauvericin in RLM for CYP2C was not evaluated in the present study.

The pharmacokinetic properties of beauvericin in rats were studied at the doses of 0.5, 1, 2 mg/kg respectively. As expected, the exposures of beauvericin in rats increased as the administration dosage increased (Figure 7(A)). Ketoconazole is a well known potent CYP3A inhibitor, giving a K_i of 0.14 μM in RLM (Salem Omran Ali Abdalla, dissertation, Department of Clinical Pharmacology, Georg-August University, Gottingen. Germany, June 2007). Ketoconazole also displayed a short half-life of 1.38 h in rats [24]. In our present study, the $AUC_{0\text{-}t}$ for beauvericin administered alone (0.5 mg/kg) and administrated simultaneously with ketoconazole (both 0.5 mg/kg) were calculated to be 27.9 h·mg·L^{-1} and 31.1 h·mg·L^{-1}, respectively, indicating no significant difference in the exposures of beauvericin in rats. Additionally with the comparison of these two administrations, C_{max} of 3.4 versus 3.8 mg·L^{-1} and T_{max} of 4.1 h versus 3.4 h did not display significantly different. Similarily, the exposures of ketoconazole were not significantly different in its administration alone and simultaneously co-administration with beauvericin. It is worthwhile to mention that the antifungal activity by a combination administration of beauvericin with ketoconazole displays more than 100-fold higher than that by a single application of either alone [2]. Our finding indicates that the synergetic effect on antifungal activities obtained with co-administration of beauvericin and ketoconazole was not caused by their pharmacokinetic interactions.

Declaration of interest: The authors report no conflicts of interest. The authors alone are responsible for the content and writing of the paper.

Notes

†Tel: 86 20 32290426. E-mail: mei_li@gibh.ac.cn
‡E-mail: lzhang03@gmail.com

References

[1] Plattner RD, Nelson PE. Production of beauvericin by a strain of *Fusarium proliferatum* isolated from Corn Fodder for Swine. Appl Environ Microbiol 1994;60:3894–3896.

[2] Zhang LX, Yan KZ, Zhang Y, Huang R, Bian J, Zheng CS, Sun HX, Chen ZH, Sun N, An R, Min FG, Zhao WB, Zhuo Y, You JL, Song YJ, Yu ZY, Liu ZH, Yang KQ, Gao H, Dai HQ, Zhang XL, Wang J, Fu CZ, Pei G, Liu JT, Zhang S, Michael G, Jiang YY, Kuai J, Zhou GC, Chen XP. High-throughput synergy screening identifies microbial metabolites as combination agents for the treatment of fungal infections. PNAS 2007;104:4606–4611.

[3] Goodman JL, Winston DJ, Greenfield RA, Chandrasekar PH, Fox B, Kaizer H, Shadduck RK, Shea TC, Stiff P, Friedman DJ. A controlled trial of fluconazole to prevent fungal infections in patients undergoing bone marrow transplantation. N Engl J Med 1992;326:845–851.

[4] Larocco MT, Burgert SJ. Infection in the bone marrow transplant recipient and role of the microbiology laboratory in clinical transplantation. Clin Microbiol Rev 1997; 10:277–297.

[5] Sanchez V, Vasquez JA, Barth-Jones D, Dembry L, Sobel JD, Zervus MJ. Nosocomial acquisition of *Candida parapsilosis*: An epidemiologic study. Am J Med 1993;94:577–582.

[6] Rex JH, Rinaldi MG, Pfaller MA. Resistance of Candida species to fluconazole. Antimicrob Agents Chemother 1995;39:1–8.

[7] Ghannoum MA, Rice LB. Antifungal agents: Mode of action, mechanisms of resistance, and correlation of these mechanisms with bacterial resistance. Clin Microbiol Rev 1999;12:501–517.

[8] Sugar AM, Alsip SG, Galgiani JN, Graybill JR, Dismukes WE, Cloud GA, Craven PC, Stevens DA. Pharmacology and toxicity of high-dose ketoconazole. Antimicrob Agents Chemother 1997;31:1874–1878.

[9] Bjornsson TD, Callaghan JT, Einolf HJ, Fischer V, Gan L, Grimm S, Kao J, King PS, Miwa G, Ni L, Kumar G, Mcleod J, Obach SR, Roberts S, Roe A, Shah A, Snikeris F, Sullivan JT, Tweedie D, Vega JM, Walsh J, Wrighton SA. The conduct of *in vitro* and *in vivo* drug-drug interaction studies: A pharmaceutical research and manufacturers of America (PhRMA) perspective. Drug Metab Dispos 2003;31:815–832.

[10] Crespi CL, Stresser DM. Fluorometric screening for metabolism-based drug-drug interactions. J Pharmacol Toxicol Meth 2000;44:325–331.

[11] Xia ZL, Ying JY, Sheng R, Zeng S, Hu YZ, Yao TW. *In vitro* metabolism of BYZX in human liver microsomes and the structural elucidation of metabolite by liquid chromatography–mass spectrometry method. J Chromatogr B 2007;857:266–274.

[12] Yao M, Zhu MS, Michael WS, Zhang HJ, Humphreys WG, Rodrigues AD, Dai R. Development and full validation of six inhibition assays for five major cytochrome P450 enzymes in human liver microsomes using an automated 96-well microplate incubation format and LC–MS/MS analysis. J Pharm Biomed Anal 2007;44:211–223.

[13] Zhong DF, Zhang SQ, Sun L, Zhao XY. Metabolism of roxithromycin in phenobarbital-treated rat liver microsomes. Acta Pharmacol Sin 2002;23:455–460.

[14] Lowry OH, Rosebrough NJ, Farr AL, Randall RJ. Protein measurement with the Folin phenol reagent. J Biol Chem 1951;193:265–275.

[15] Kobayashi K, Urashima K, Shimada N, Chiba K. Substrate specificity for rat cytochrome P450 (CYP) isoforms: Screening with cDNA-expressed systems of the rat. Biochem Pharmacol 2002;63:889–896.

[16] Obach SR, Reed-Hagen AE. Measurement of Michaelis Constants for cytochrome P450-mediated biotransformation reactions using a substrate depletion approach. Drug Metab Dispos 2002;30:831–837.

[17] Nath A, Atkins WM. A theoretical validation of the substrate depletion approach to determining kinetic parameters. Drug Metab Dispos 2006;34:1433–1435.

[18] Segal IH. Enzyme kinetics. New York: Wiley-Interscience; 1975. p 957.

[19] Chang TK, Chen J, Lee WB. Differential inhibition and inactivation of human CYP1 enzymes by *trans*-resveratrol: Evidence for mechanism-based inactivation of CYP1A2. J Pharmacol Exp Ther 2001;299:874–882.
[20] Zhang D, Zhu M, Humphreys WG. Drug metabolism in drug design and developmen. New Jersey: Wiley; 2007. p 513–543.
[21] Rodriques D. Drug-drug interactions. New York: Marcel Dekker, Inc; 2002. p 217–293.
[22] Lee JS, Obach RS, Fisher MB. Drug metabolizing enyzmes: Cytochrome P450 and other enzymes in drug discovery and development. New York: Fontis Media, Lausanne, Switzerland and Marcel Dekker; 2003. p 211–254.
[23] Jones HM, Houston JB. Substrate depletion approach for determining *in vitro* metabolic clearence: Time dependences in hepatocyte and microsomal incubations. Drug Metab Dispos 2004;32:973–982.
[24] Kotegawa T, Laurijssens BE, Durol ALB, Greenblatt DJ. Pharmacokinetics and electroencephalographic effects of ketoconazole in the rat. Biopharm Drug Dispos 1999; 20:49–52.